

This is the Accepted Author Manuscript of the publication

Longitudinal monitoring of metabolic alterations in cuprizone mouse model of multiple sclerosis using 1H-magnetic resonance spectroscopy.

Jasmien Orije^a, Firat Kara^a, Caroline Guglielmetti^a, Jelle Praet^a, Annemie Van der Linden^a, Peter Ponsaerts^b, Marleen Verhoye^a

^a Bio-Imaging Lab, University of Antwerp, Antwerp, Belgium

^b Experimental Cell Transplantation Group, Laboratory of Experimental Hematology, University of Antwerp, Antwerp, Belgium

Corresponding author:

F. Kara

fiat.kara@uantwerpen.be

Published in: Neuroimage. 2015 Jul 1;114:128-35.

Doi: 10.1016/j.neuroimage.2015.04.012

The final publication is available at

<http://www.sciencedirect.com/science/article/pii/S105381191500302X>

Longitudinal monitoring of metabolic alterations in cuprizone mouse model of multiple sclerosis using ¹H-magnetic resonance spectroscopy

Jasmien Orije^{a,1}

Firat Kara^{a,*,1}

firat.kara@uantwerpen.be

Caroline Guglielmetti^a

Jelle Praet^a

Annemie Van der Linden^a

Peter Ponsaerts^b

Marleen Verhoye^a

^aBio-Imaging Lab, University of Antwerp, Antwerp, Belgium

^bExperimental Cell Transplantation Group, Laboratory of Experimental Hematology, University of Antwerp, Antwerp, Belgium

*Corresponding author at: Bio-Imaging Lab, University of Antwerp, Department of Biomedical Sciences, Campus Drie Eiken, D.UC.109, Universiteitsplein 1, B2610 Wilrijk, Belgium. Fax: + 32 32652774.

¹The authors contributed equally to this manuscript.

Abstract

Non-invasive measures of well-known pathological hallmarks of multiple sclerosis (MS) such as demyelination, inflammation and axonal injury would serve as useful markers to monitor disease progression and evaluate potential therapies. To this end, in vivo localized proton magnetic resonance spectroscopy (¹H-MRS) provides a powerful means to monitor metabolic changes in the brain and may be sensitive to these pathological hallmarks. In our study, we used the cuprizone mouse model to study pathological features of MS, such as inflammation, de- and remyelination, in a highly reproducible manner. C57BL/6J mice were challenged with a 0.2% cuprizone diet for 6-weeks to induce demyelination, thereafter the mice were put on a cuprizone free diet for another 6 weeks to induce spontaneous remyelination. We employed in vivo ¹H-MRS to longitudinally monitor metabolic changes in the corpus callosum of cuprizone-fed mice during the demyelination (weeks 4 and 6) and spontaneous remyelination (week 12) phases. The MRS spectra were quantified with LCModel and since the total creatine (tCr) levels did not change over time or between groups, metabolite concentrations were expressed as ratios relative to tCr. After 4 and 6 weeks of cuprizone treatment a significant increase in

taurine/tCr and a significant reduction in total N-acetylaspartate/tCr, total choline-containing compounds/tCr and glutamate/tCr could be observed compared to mice under normal diet. At week 12, when almost full remyelination was established, no statistically significant metabolic differences were present between the control and cuprizone group. Our results suggest that these metabolic changes may represent sensitive markers for cuprizone induced demyelination, axonal injury and inflammation. To the best of our knowledge, this is the first longitudinal in vivo ¹H-MRS study that monitored biochemical changes in the corpus callosum of cuprizone fed mice.

Abbreviations: ¹H-MRS, proton magnetic resonance spectroscopy; Cho, choline; CNS, central nervous system; CPZ, cuprizone; GABA, γ -aminobutyric acid; CNS, central nervous system; f_{csf} , volume fraction of cerebrospinal fluid; f_{gm} , volume fraction of gray matter; f_{wm} , volume fraction of white matter; Glc, glucose; Glu, glutamate; Gln, glutamine; Glx, Glu + Gln; GSH, glutathione; GPC, glycerophosphorylcholine; Lip, lipid; LSD, least significant difference; mIns, *myo*-inositol; MS, multiple sclerosis; MR, magnetic resonance; MRI, magnetic resonance imaging; NAA, N-acetylaspartate; NAAG, N-acetylaspartylglutamate; OPC, oligodendrocyte progenitor cells; PCho, phosphorylcholine; PCr, phosphocreatine; OVS, outer volume suppression; RARE, rapid acquisition and relaxation enhancement; sIns, *scyllo*-inositol; Tau, taurine; tCho, total choline (GPC + Cho); tCr, total creatine; TE, echo time; tNAA, NAA + NAAG; TR, repetition time; VOI, volume of interest

Keywords: Cuprizone mouse model; Proton magnetic resonance spectroscopy; Longitudinal; Multiple sclerosis; Demyelination; Remyelination

Introduction

Multiple sclerosis (MS) is a chronic immune-mediated demyelinating disease of the central nervous system (CNS) affecting about 2 million people worldwide (Denic et al., 2011). The main neuropathological hallmarks of MS are focal demyelination, inflammation and reversible axonal damage (Lucchinetti et al., 2005). Definite evidence of these hallmarks in MS is mainly obtained from *post-mortem* studies (Kolasinski et al., 2012; Lucchinetti et al., 2000). However, the in vivo detection of these changes and their underlying mechanisms is challenging. Magnetic resonance (MR) based techniques provide a non-invasive means to investigate these features of MS pathology in vivo. Although conventional MR imaging (MRI) techniques are sensitive to changes in myelin integrity, these techniques cannot discriminate between inflammation, demyelination and axonal injury (Laule et al., 2007). Thus, to obtain a better insight into the underlying pathology, and to evaluate the success of new therapeutic strategies, there is an emergent need for specific and sensitive in vivo MR-based techniques.

To this end, localized proton magnetic resonance spectroscopy ($^1\text{H-MRS}$) serves as a novel technique, which provides metabolic information on various aspects of in vivo neurochemistry, including neuroaxonal integrity, gliosis and energy metabolism (De Stefano et al., 2005; Duarte et al., 2012). For example, the amount of N-acetylaspartate (NAA)/total Creatine (tCr) ratio has been proposed as a marker of neuroaxonal integrity (Choi et al., 2007; De Stefano and Filippi, 2007). In addition, by measuring choline-containing metabolites and taurine (Tau), $^1\text{H-MRS}$ has provided information regarding membrane turnover and osmotic stress respectively. Although $^1\text{H-MRS}$ markers are valuable to gain a greater insight into the disease progression, application of $^1\text{H-MRS}$ is currently limited to clinical trials and experimental studies (Supplementary Table S1) and rarely applied as a diagnostic tool (Filippi et al., 2013). Moreover, the use of $^1\text{H-MRS}$ in MS patients is limited by the heterogeneity between MS patients and the inconvenience to histologically validate the pathology. In contrast, animal models enable us to study pathological features of MS, such as demyelination, remyelination and inflammation in a more reproducible manner. However, so far only few animal studies focused on the detection of these pathological features using $^1\text{H-MRS}$ (Supplementary Table S2). Among these animal models, the CPZ mouse model is a well-characterized model of MS. This model mimics the primary oligodendroglial pathology associated demyelination as seen in type III/IV MS lesions (Denic et al., 2011; Lucchinetti et al., 2005). CPZ fed mice present a well-established and reproducible spatiotemporal pattern of inflammation, de- and remyelination in white matter tracts such as the corpus callosum. The copper chelating properties of CPZ cause mitochondrial and metabolic stress to oligodendrocytes, which eventually lead to oligodendrocyte loss and demyelination during the first weeks of CPZ administration (Kipp et al., 2009; Skripuletz et al., 2011). The demyelination in the corpus callosum is associated with a variety of factors such as gliosis and macrophages (Gudi et al., 2009). During 6 weeks of CPZ treatment oligodendrocyte progenitor cells (OPC) accumulate and start spontaneous remyelination, which is further continued when CPZ is withdrawn from the diet at week 6 (Mason et al., 2000; Morell et al., 1998; Stidworthy et al., 2003). This highly reproducible, distinct de- and remyelination of the corpus callosum makes the CPZ-treated mice an ideal model to longitudinally monitor changes in the white matter (Lindner et al., 2008; Matsushima, 2001). While much is known about CPZ-induced demyelination, longitudinal in vivo biochemical fingerprinting of CPZ-induced demyelination in the corpus callosum with $^1\text{H-MRS}$ has not been attempted yet. In vivo metabolic changes detected with $^1\text{H-MRS}$ can provide better insight into some of the pathological features of MS such as demyelination and remyelination.

The aim of this study was to: (1) obtain a metabolic fingerprint of the corpus callosum of the CPZ-treated mice with in vivo $^1\text{H-MRS}$; (2) longitudinally follow, in vivo metabolic

changes in the corpus callosum of CPZ fed mice in order to get better insight into how dynamic changes of several metabolites can reflect inflammation, neuroaxonal suffering, de- and remyelination using in vivo ¹H-MRS; and (3) follow histological changes in CPZ fed mice in order to validate inflammation, de- and remyelination.

Materials and methods

CPZ treatment and experimental groups

All procedures were performed in accordance with the European guidelines for the care and use of laboratory animals (Directive 2010/63/EU) and were approved by the Committee on Animal Care and Use at the University of Antwerp, Belgium (2013-57).

Female C57BL/6 mice, 8 weeks of age, were obtained from Charles River Laboratories (strain code 027) and divided into a CPZ (N = 15) and control group (N = 15). The mice of the CPZ group were fed standard lab chow mixed with 0.2% (w/w) CPZ (Sigma-Aldrich, Germany) for a period of 6 weeks, thereafter mice were returned to a cuprizone-free rodent chow and remained on this diet for another 6 weeks. The control mice were maintained on normal rodent chow. Mice were housed in a 12 h light/dark cycle with ad libitum access to food and water. Eighteen additional female C57BL/6 mice were used for histological evaluation of the CPZ mouse model. For each time point (weeks 4, 6 and 12) three CPZ-treated and three control mice were sacrificed.

Magnetic resonance spectroscopy

All MR-based measurements were performed on a 9.4 Tesla Biospec scanner with a horizontal bore (20 cm in diameter) (Biospec 94/20 USR, Bruker Biospin, Germany), equipped with a standard Bruker crosscoil setup using a quadrature volume coil for excitation and quadrature mouse surface coil for signal detection (Bruker Biospin, Ettlingen, Germany). The system was interfaced to a Linux PC running Topspin 2.0 and Paravision 5.1 software (Bruker Biospin).

For MR studies, all mice were initially anesthetized using 3% isoflurane and maintained at 2% isoflurane (Forane Abnott, UK) in a mixture of 30% O₂ and 70% N₂ at a flow rate of 600 ml/min. The anesthetic gas was administered via a special facemask with a tooth bar, which kept the mouse head immobile. Throughout the MR studies, respiration rate was constantly monitored by a pressure sensitive respiration sensor, placed under the abdomen. Body temperature was monitored with a rectal temperature probe and was maintained at 37.0 ± 0.5 °C using a warm air system with a feedback unit (SA Instruments, NY, USA). The respiration and body temperature control systems were connected to a computer with pcSam monitoring software (SA Instruments, NY, USA).

The volume of interest (VOI) for ^1H -MRS was localized using multislice rapid acquisition and relaxation enhancement (RARE) images (Hennig et al., 1986). The RARE images were acquired in three orthogonal directions (axial, coronal and sagittal) with following parameters: repetition time (TR) = 2500 ms, echo time (TE) = 33.442 ms, matrix size (256 × 56), field of view = (20 × 20) mm², 16 slices, slice thickness = 0.4 mm, RARE factor = 8. A VOI (0.9 mm × 2.5 mm × 1 mm = 2.25 mm³) was placed in the splenium of corpus callosum of the mouse brain (Fig. 1). Consistent voxel placement for ^1H -MRS was achieved in each mouse by using anatomical markers such as the hippocampus, cortex and third ventricle in three orthogonal RARE slices. The volume fractions of cerebrospinal fluid (f_{csf}), gray and white matter (f_{gm} and f_{wm}) within the VOI for ^1H -MRS were estimated manually from the T2-weighted RARE images using an image analysis software (i.e. Amira 5.4). These volume fractions were used to assess reposition accuracy between scans and subjects. Furthermore, they allowed us to perform a partial volume correction to determine accurate absolute total creatine (tCr) concentrations. FASTMAP was employed to automatically adjust first- and second-order shim coils for the VOI (Gruetter, 1993; Tkac et al., 2004). Spectral line widths of water around 18–20 Hz were obtained. In vivo localized ^1H MR spectra were acquired with a point resolved spectroscopy sequence in combination with outer volume suppression (OVS) and VAPOR water suppression (Bottomley, 1987; Tkac et al., 1999). There was no gap between OVS and voxel. The following parameters were used: TR = 4000 ms, TE = 15 ms, number of averages = 720, water (4.7 ppm) as frequency on resonance, spectral width = 4006 Hz or 10 ppm, number of acquired points = 2048 yielding a spectral resolution of 0.98 Hz/pt. The total acquisition time amounted to 48 min. For each animal, an unsuppressed water signal (TE = 15 ms, TR = 4000 ms, 64 averages, scanning time = 5 min, VAPOR and OVS turned off) was acquired immediately after acquiring the water-suppressed spectrum. During post-processing, this unsuppressed water signal was used for Eddy-current correction by the LCModel, where the water suppressed MRS signal (in time domain) is point-wise divided by the phase part of the unsuppressed water signal (Mandal, 2012). An unsuppressed water spectrum (TE = 15 ms, TR = 4000 ms, number of averages = 1) was acquired before and after each ^1H -MRS spectrum (water suppressed) for frequency drift estimation. These two unsuppressed water spectra were analyzed by Bruker's TopSpin™ software package to estimate the level of frequency drift.

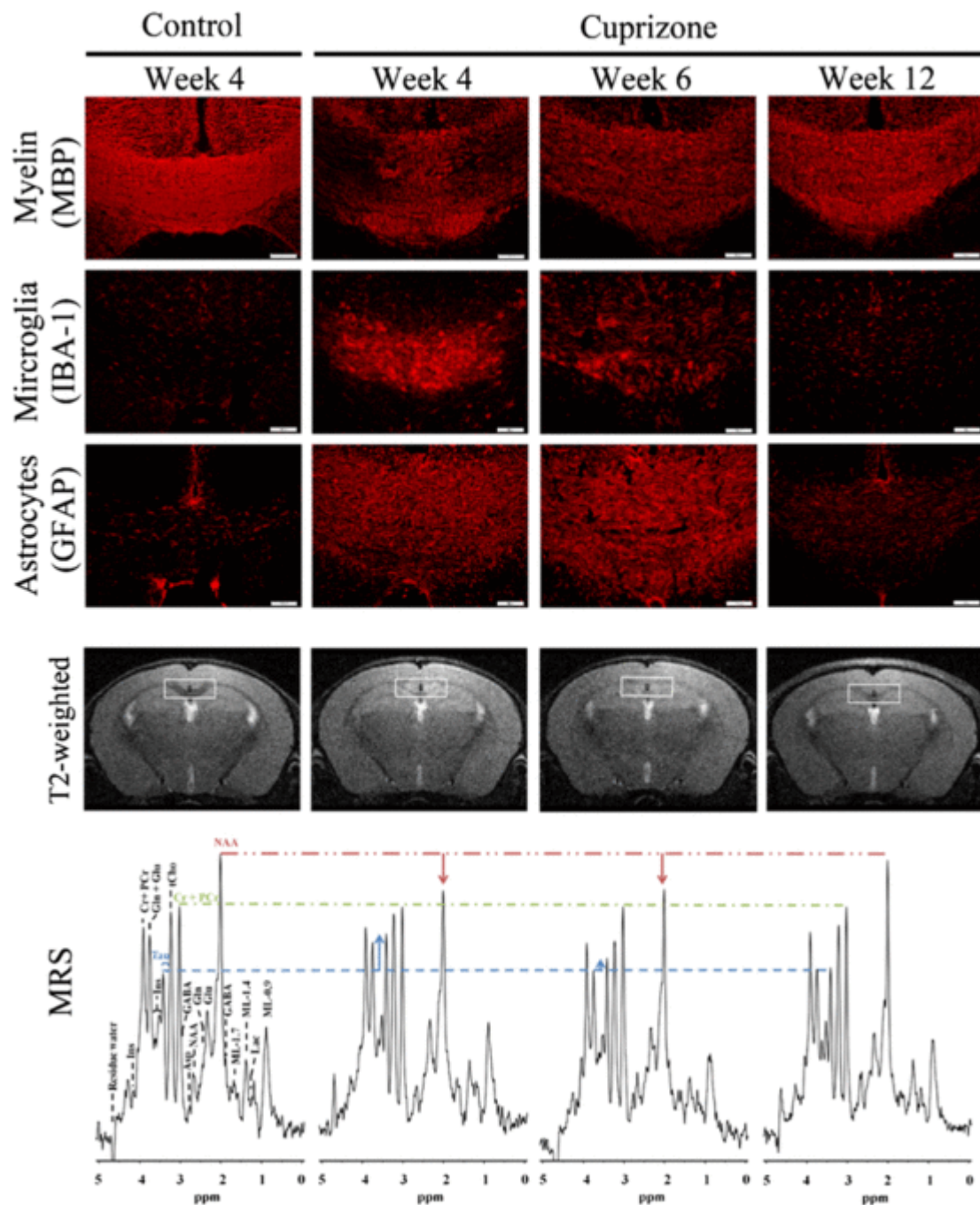


Fig. 1 Representative overview of histology, axial T2-weighted images and localized spectra obtained from the corpus callosum of control and CPZ-treated mice at weeks 4, 6 and 12 (6 weeks after returning to normal diet). Histology shows the amount of myelin (MBP staining), microgliosis (IBA-1 staining) and astrogliosis (GFAP staining) present at these different time points. During acute demyelination (week 4), extensive microgliosis and astrogliosis can be observed. By week 6 of CPZ intoxication, an attempt of remyelination is visible while astrogliosis persists in the absence of microgliosis. 6 weeks after returning to normal diet, spontaneous remyelination occurs, while microgliosis and astrogliosis have disappeared. Hyperintense lesions at the level of the corpus callosum are observed in the T2-weighted images at weeks 4 and 6, which also reflect the ongoing demyelination and

inflammation. At week 12 these hyperintensities are no longer observed. ^1H MR spectra are obtained from VOIs positioned at the splenium of the corpus callosum, designated as white boxes in the corresponding T2-weighted images above. Longitudinal alterations in NAA and Tau levels are shown with arrows.

^1H MR spectra were acquired using the same control and CPZ-treated mice at 3 different time points: week 4 and week 6 (to observe demyelination and inflammation) and week 12 (to observe remyelination).

Metabolite quantification using LCModel

In vivo ^1H MR spectra were analyzed using an automated deconvolution program (LCModel) (Provencher, 2001) as described previously (Marjanska et al., 2005; Oz et al., 2010; Tkac et al., 2004). Quantification with the LCModel is not user biased and performs many corrections like spectral phasing automatically. The LCModel analysis was performed within the chemical shift range of 0.2–4.2 ppm. The following metabolites were included in the basis set of the LCModel: alanine, aspartate, creatine (Cr), phosphocreatine (PCr), γ -aminobutyric acid, glucose (Glc), glutamate (Glu), glutamine (Gln), glutathione (GSH), glycerophosphorylcholine (GPC), phosphorylcholine (PCh), Inositol (Ins), lactate, N-acetylaspartate (NAA), N-acetylaspartylglutamate (NAAG), *scyllo*-inositol and taurine (Tau). Besides this standard set of brain metabolites, LCModel includes 9 stimulated macromolecule and lipid peaks (Pfeuffer et al., 1999).

The reliability of the metabolite quantification was assessed using the Cramér-Rao lower bounds (CRLB, estimated error of quantification) provided by the LCModel. Stringent selection criteria were applied as follows: metabolites quantified with $\text{CRLB} > 20\%$ were classified as not detected, and metabolites with $\text{CRLB} \leq 20\%$ in at least 50% of the spectra were included in the neurochemical profile. Frequency drift in spectra was less than 0.04 ppm on average. In most spectra, the present analysis was unable to reliably discern PCh from GPC, NAA from NAAG or Cr from PCr. More accurate are the sums expressed as total choline-containing compounds (GPC + PCh or tCho), total NAA (NAA + NAAG or tNAA) and tCr (Cr + PCr) respectively. Due to the higher field, Glu and Gln could be quantified individually with good accuracy, but the combined Glu and Gln (Glx) concentration was also determined.

Absolute tCr concentrations (in $\mu\text{mol/g}$) were determined relative to an unsuppressed water signal acquired from the same VOI. In addition, absolute tCr concentrations were corrected for partial volume effects by taking the volume fractions of white and gray matter into account in the quantification (Provencher, 1993). These volume fractions were used to correct the total water concentration for each VOI using the following equation: water concentration = $(43300f_{\text{gm}} + 35880f_{\text{wm}} + 55556f_{\text{csf}})/(1-f_{\text{csf}})$ (Provencher, 2014). Since the absolute

tCr concentrations did not change over time or between groups in our study (data not shown), we express our metabolite concentrations relative to tCr, as concentration ratios are less sensitive to relaxation and partial volume effects (Provencher, 1993, 2001).

Histological analysis

For histological analysis, mice (additional subset of mice, 3 per time point and group) were deeply anesthetized via an intraperitoneal injection of 60 mg/kg/BW pentobarbital (Nembutal, Ceva Sante Animale), transcardially perfused with 0.9% NaCl and perfused-fixed with 4% paraformaldehyde. Whole brains were surgically removed and post-fixed in 4% paraformaldehyde for 2 h. Fixed brains were freeze-protected via a sucrose gradient (2 h at 5%, 2 h at 10% and overnight at 20%), snap frozen in liquid nitrogen and stored at -80°C until further processing. Consecutive 10 μm -thick cryosections were prepared using a microm HM500 cryostat at the level of the splenium. For immunofluorescence analysis of microgliosis, astrogliosis and myelin quantity the following antibodies were used respectively: a rabbit anti-mouse IBA1 antibody (Wako, 019-19741; 1/200 dilution) in combination with an Alexa Fluor® 555-labeled donkey anti-rabbit secondary antibody (Invitrogen, A31572; 1/1000 dilution), a mouse anti-GFAP antibody (Millipore bioscience, MAB360; 1/400 dilution) in combination with an Alexa Fluor® 555-labeled goat anti-mouse secondary antibody (Invitrogen, A21127; 1/1000 dilution) and a chicken anti-MBP antibody (Millipore, AB9348; 1/200 dilution) in combination with a DyLight549 donkey anti-chicken secondary antibody (Jackson ImmunoResearch, 703-506-155; 1/1000 dilution). Slides were mounted using Prolong Gold Antifade (Invitrogen, P36930). Immunofluorescence images were acquired using a standard research fluorescence microscope (Olympus Bx51 fluorescence microscope) equipped with an Olympus DP71 digital camera. Olympus CellSense software was used for image acquisition.

Statistical analysis

The variability of metabolic measurements over time was assessed with the coefficient of variation calculated from control mice ($n = 8$) scanned at 4, 6 and 12 weeks. The coefficient of variation is defined as the ratio of the standard deviation of metabolite/tCr to the mean of metabolite/tCr. In addition, the coefficients of variation of the partial volume fractions were assessed to estimate the repositioning accuracy.

Metabolic data was first analyzed with linear mixed model, with 'Group', 'Time' and their interaction 'Group \times Time' used as fixed factors. This analysis identified which metabolites were significantly different between groups, and which metabolites changed significantly over time. Next, significant group differences of individual metabolites per time point were identified using a two-tailed Student's t-test. P-values were Bonferroni corrected for multiple comparisons between three time points.

Subsequently, longitudinal metabolic changes over the different time points were quantified using a linear mixed model with post hoc Bonferroni analysis for both groups separately. The threshold for statistical significance of the linear mixed model was set at $p < 0.05$.

Results

Validation of the CPZ mouse model

First, we used immunohistochemistry (Fig. 1) to validate the reproducibility of the CPZ mouse model by visual assessment of the extent of demyelination (MBP staining) and inflammation characterized by microgliosis and astrogliosis (IBA-1 and GFAP staining, respectively). Control animals presented a fully myelinated corpus callosum without signs of inflammation, whereas 4 weeks of CPZ treatment resulted in severe demyelination of the corpus callosum along with extensive microgliosis and astrogliosis. After 6 weeks of CPZ treatment the level of demyelination and microgliosis was markedly decreased. In contrast, astrocyte reactivity persisted throughout CPZ treatment. Six weeks after returning to a normal diet, microgliosis and astrogliosis activity were no longer visible, which was accompanied by spontaneous remyelination in the corpus callosum.

Neurochemical profiles obtained with ^1H -MRS

High quality ^1H MR spectra with good resolution, high signal-to-noise ratio and a flat baseline were acquired from a VOI centered in the splenium of the corpus callosum (see Fig. 1, and Inline Supplementary Figure S1). On average the white matter and gray matter accounted for $34 \pm 4\%$ and $65 \pm 4\%$ of the VOI respectively. There was no contribution of cerebrospinal fluid fraction in any of the VOIs. Variation in the partial volume fractions f_{wm} and f_{gm} due to manual reposition of the VOI was only 8% and 4% respectively, suggesting that the voxel placement was consistent. The average coefficient of variation obtained from repeated measurements (weeks 4, 6 and 12) in control mice was summarized in Table 1. No statistically significant change ($p > 0.05$) was observed in the absolute concentration of tCr ($\mu\text{mol/g}$) between the control and CPZ group at any time point. Due to the high spectral quality, longitudinal neurochemical alterations of NAA and Tau were discernible in individual spectra (Fig. 1). The corpus callosum of control mice appeared hypointense in T2-weighted images, whereas the corpus callosum of CPZ fed mice presented hyperintensities at weeks 4 and 6, indicative of inflammation and/or demyelination. At week 12, 6 weeks after CPZ withdrawal, no differences were observed between intensities of the corpus callosum of CPZ fed mice and control mice.

Inline Supplementary Fig. S1 can be found online at <http://dx.doi.org/10.1016/j.neuroimage.2015.04.012>.

Metabolic alterations due CPZ-induced pathology

Metabolic profiles of the corpus callosum of control and CPZ-treated mice are depicted in [Fig. 2](#) and [Table 1](#). Additionally, [Table 1](#) shows the number of animals included at each time point and the average CRLB values of metabolites. A linear mixed model was used to evaluate the treatment effect, the longitudinal changes and their interaction (see [Inline Supplementary Table S3](#)). For given metabolites Glc, Glu, Glx, Ins, Tau, tCho and tNAA a significant group effect was observed ($p < 0.05$). In addition, a significant time effect was observed in GSH/tCr, Glu/tCr, tCho/tCr and tNAA/tCr ratios ($p < 0.01$). Tau/tCr and tNAA/tCr ratios also showed a significant interaction between time and group ($p < 0.05$) (see [Inline Supplementary Table S3](#)). Next, an in-depth group analysis per time point revealed significant neurochemical alterations in the corpus callosum of CPZ fed mice compared to control mice at 4 and 6 weeks of the treatment ([Fig. 2](#), [Table 1](#)). At both weeks 4 and 6, tNAA/tCr, tCho/tCr and Glu/tCr ratios were significantly lower while Tau/tCr ratios were significantly higher in CPZ fed mice compared to control mice. Furthermore, the Glc/tCr and Glx/tCr ratios were significantly lower in the CPZ group compared to the control group at week 4 ([Table 1](#)). Six weeks after CPZ withdrawal (at week 12), no statistically significant metabolic differences ($p > 0.05$) were observed between both groups.

[Inline Supplementary Table S3](#) can be found online at <http://dx.doi.org/10.1016/j.neuroimage.2015.04.012>.

Time courses of metabolite levels revealed different trends in CPZ exposed mice compared to control mice ([Fig. 3](#)). An additional linear mixed model analysis was applied to verify the significance of the time effect in each group separately ([Table 2](#)). The control group showed a significant metabolic change in Glu/tCr and GSH/tCr ratios over time ([Fig. 3](#)). CPZ-treated mice depicted significant longitudinal changes in Tau/tCr ($p < 0.001$), tCho/tCr ($p < 0.001$) and tNAA/tCr ($p < 0.01$) ratios ([Table 2](#)). A post hoc Bonferroni comparison revealed significant differences ($p < 0.05$) between different time points for Tau/tCr; tCho/tCr, tNAA/tCr, Glu/tCr, and GSH/tCr ([Fig. 3](#) and [Table 2](#)). Neither the control nor CPZ-treated group presented a longitudinal change in Glc/tCr ratios.

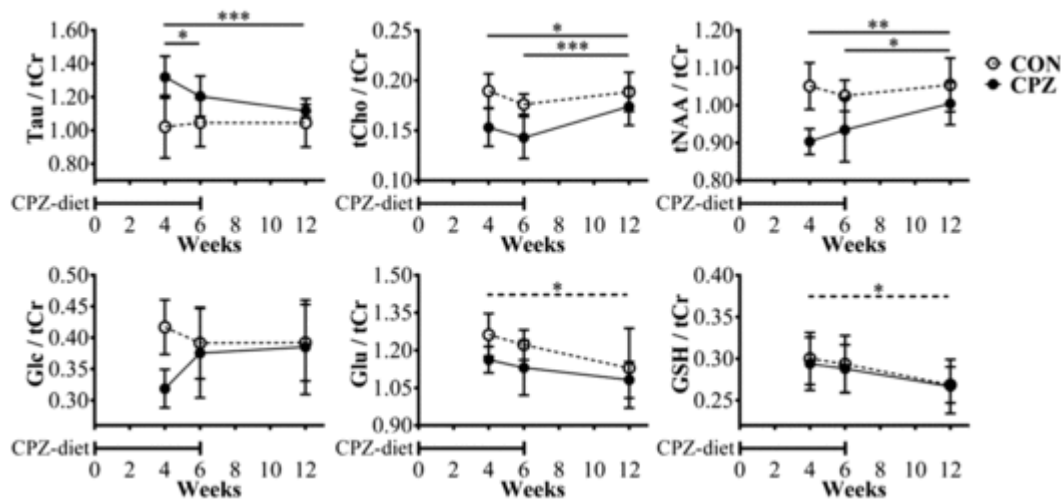


Fig. 3 Time courses of mean metabolite concentrations relative to tCr acquired from VOI containing the corpus callosum of CPZ-treated and control mice. Statistical analysis with linear mixed model with post hoc Bonferroni analysis revealed significant longitudinal differences of metabolites in the control (CON, dashed lines) and CPZ-treated group (full lines) and are indicated by * ($p < 0.05$), ** ($p < 0.01$) or *** ($p < 0.001$). Error bars shown are the standard deviation.

Table 2 Significant longitudinal metabolic alterations in the control and CPZ-treated group revealed by statistical analysis with linear mixed model.

	Time effect	Post hoc Bonferroni		
		w4 vs. w6	w4 vs. w12	w6 vs. w12
<i>CON</i>				
Glu/tCr	$p < 0.05$		$p < 0.05$	
GSH/tCr	$p < 0.05$		$p < 0.05$	
<i>CPZ</i>				
Tau/tCr	$p < 0.001$	$p < 0.05$	$p < 0.001$	
tCho/tCr	$p < 0.001$		$p < 0.05$	$p < 0.001$
tNAA/tCr	$p < 0.01$		$p < 0.01$	$p < 0.05$

P-values indicate a significance level of difference between time point week 4 and week 6, week 4 and week 12, and week 6 and week 12. Only p values, which indicate a significant difference across the time points, are depicted.

The pathological alterations, such as gliosis and demyelination, in CPZ-treated mice were most severe at week 4. Therefore, the major alterations in the metabolic ratios seen in

CPZ-treated mice may reflect the pathological severity. In particular, a statistically significant increased level of Tau/tCr ratio was observed at week 4 compared to week 6, suggesting that the Tau/tCr ratio may indicate the severity of the CPZ pathology. Interestingly, when almost full remyelination was observed at week 12, no statistically significant differences were observed between metabolite ratios of control and CPZ-treated mice.

Discussion

In the CPZ mouse model, longitudinal monitoring of *in vivo* changes in regional metabolites within the brain has not been attempted so far. We employed quantitative *in vivo* ^1H -MRS to longitudinally monitor brain metabolic changes in the corpus callosum of the C57BL/6 mice, which were challenged with CPZ diet for 6 weeks followed by a recovery phase of 6 weeks with a cuprizone-free diet. Doing so we investigated how some of the neurochemical changes in the brain reflect demyelination, axonal damage and/or gliosis, and spontaneous remyelination.

Longitudinal ^1H -MRS analysis

In this longitudinal study, we demonstrated *in vivo* metabolic changes at the level of the corpus callosum of CPZ fed mice. The major finding of our study was a reversible and significant decrease in the ratio of tNAA/tCr in CPZ-treated mice during demyelination, reflecting reversible axonal injury due to CPZ treatment. The observed alterations of the tNAA/tCr ratio during demyelination and spontaneous remyelination, were well in line with prior longitudinal studies in MS patients (Davie et al., 1994; Kirov et al., 2013; Mader et al., 2000) and MS animal models (Denic et al., 2009) (see Table S1 and Table S2). Interestingly a reversible increase in Tau/tCr ratio was observed in our study. However, MS patients exhibited increased levels of mIns rather than increased Tau levels (Kirov et al., 2013). Since both mIns and Tau function as an osmoregulator, an increased Tau/tCr ratio in mice may reflect a similar process as the one responsible for a mIns increase in human patients (Dedeoglu et al., 2004). In addition, Tau is found in a much higher concentration in the rodent brain compared to the human brain, which makes it easier to detect compared to mIns. Similar to our results, elevated Tau concentrations were observed in other animal models, where white matter integrity was decreased (Bucur et al., 2008; Choi et al., 2009; Dedeoglu et al., 2004).

The interpretation of the reversible decrease in the signal of choline containing compounds during the demyelination phase is complicated. Some MS studies reported an increased level of choline containing compounds (Bitsch et al., 1999; Tourbah et al., 1996), while others reported unchanged or reduced tCho levels (Chard et al., 2002; Davies et al., 1995; Gustafsson et al., 2007; Oh et al., 2004; Sijens et al., 2006). Since CPZ causes mitochondrial dysfunction (Venturini, 1973), it may disturb the energy metabolism (Kipp et al., 2009). In line with our results, a decrease in choline containing compounds has been reported in studies of

patients with mitochondrial diseases (Bianchi et al., 2003; De Stefano et al., 1995; Saneto et al., 2008). In addition Xuan et al. (2014) recently reported that CPZ exposure even for a short period causes a decrease in GPC + PCho levels, presumably due to the mitochondrial impairment.

In our study, linear mixed model analysis revealed significant group and time effects in the Glu/tCr ratio. In MS patients Glu concentrations are often increased in acute MS lesions (Srinivasan et al., 2005), whereas they are often decreased in cortical gray matter (Chard et al., 2002; Ramadan et al., 2013). The elevated levels of Glu in acute MS lesions are often linked to glutamate excitotoxicity induced by inflammation. The decrease in Glu/tCr ratio could be linked to the CPZ induced mitochondrial dysfunction, as impaired mitochondrial function can be correlated to decreased Glu levels (Boumezbeur et al., 2010). Furthermore, a recent study, investigating the expression of Glu receptors and transporters during CPZ treatment, showed increased expression of the Glu transporter GLAST in the corpus callosum of CPZ treated mice. They suggested that due to the chronic exposure to CPZ, a long lasting change in GLAST expression might be effective in coping with glutamate toxicity (Azami Tameh et al., 2013).

In line with other longitudinal MRS studies, a significant decrease of GSH (Duarte et al., 2014) and Glu (Boumezbeur et al., 2010; Duarte et al., 2014) was observed over time in the control group. The interpretation of alterations in Glu/tCr ratio observed in this study is complicated as isoflurane anesthesia can alter glucose homeostasis (Duarte and Gruetter, 2012; Kofke et al., 1987).

Evaluation of microstructural changes and their relation to neurochemical alterations in CPZ fed mice

In this study, extensive reversible demyelination and gliosis were observed in the corpus callosum after 4 weeks of CPZ treatment, as reported previously (Gudi et al., 2009; Lindner et al., 2008; Matsushima, 2001; Skripuletz et al., 2011). Being a putative marker of neuroaxonal integrity, a decrease in the NAA/tCr ratio reflects the presence of axonal injury caused by demyelination and gliosis. In our study we observed a significant NAA/tCr ratio change between week 4 and week 6 in CPZ-treated mice. Prior electron microscopy studies on CPZ-treated mice showed a mean reduction in axonal diameter with the presence of reversible axonal injury, characterized by swollen dystrophic axons but without significant axonal loss (Lindner et al., 2009; Lindner et al., 2008; Mason et al., 2001; Stidworthy et al., 2003; Xie et al., 2010). In line with earlier studies, a recovery of the myelin content was observed at week 6 of CPZ treatment, indicating that remyelination had already started before CPZ withdrawal (Gudi et al., 2009; Lindner et al., 2008). This early remyelination is in accordance with prior studies reporting an accumulation of oligodendrocyte progenitor cells (OPCs) in the corpus callosum at 4 and 4.5 weeks of CPZ exposure (Mason et al., 2000; Morell et al.,

1998; Skripuletz et al., 2011). These OPCs account for the reappearance of adult remyelinating oligodendrocytes between 5 and 6 weeks of CPZ treatment when they mature (Gudi et al., 2009; Lindner et al., 2008; Matsushima, 2001; Skripuletz et al., 2011). Together with the attenuated microglial activity and the beneficial role of reactive astrocytes (Lukovic et al., 2014), adult oligodendrocytes may improve neuroaxonal integrity, which could explain the gradual recovery of NAA/tCr ratios at week 6 compared to week 4.

Tau is an osmolyte to which many functions in the CNS have been ascribed, including neurotransmission, neuromodulation and neuroprotection (Burg et al., 1997; Foos and Wu, 2002; Tkac et al., 2007). The elevated Tau/tCr ratio, observed at weeks 4 and 6, may reflect an adaptive metabolic response to the hypo-osmolarity caused by the edema, which is associated with extensive inflammation (Pascual et al., 2007). It was shown that the release of Tau by astrocytes could be increased as a neuroprotective response to hypoxia, ischemia, hypo-osmolarity, oxidative stress and metabolic toxins such as CPZ (Foos and Wu, 2002; Tkac et al., 2007). Thus, an increased Tau/tCr ratio observed in this study might reflect an osmotic and neuroprotective reaction against the extensive inflammation due to CPZ exposure.

¹H-MRS can detect metabolites that play a role in cell membrane turnover, such as choline containing components (e.g. GPC and PCho). In the present study, a decrease in GPC/tCr ratio was observed during CPZ treatment, which may be linked to a variety of factors. For example, the mitochondrial impairment, caused by the copper chelating properties of CPZ, may reduce energy production, which is essential for membrane turnover (Bianchi et al., 2003; Chard et al., 2002; De Stefano et al., 1995; Saneto et al., 2008). Another possibility is that uptake of Cho from the free phase is increased as a protective response against CPZ toxicity to maintain myelin sheath integrity (Gustafsson et al., 2007). Furthermore, OPCs, which infiltrate the corpus callosum starting at week 3 of CPZ treatment (Matsushima, 2001), might further contribute to the reduction in tCho/tCr level as Cho is used for membrane formation.

It is remarkable that 6 weeks after CPZ withdrawal, when almost full remyelination has occurred no metabolic differences were observed between control and CPZ-treated mice. Even though remyelination is almost complete, CPZ treatment can result in long lasting behavioral deficits. For example motor-coordination remains affected even after 6 weeks CPZ withdrawal (Franco-Pons et al., 2007).

It should be noted that performing ¹H-MRS in a mouse brain has several limitations, such as the need for a small voxel to minimize partial volume effects, resulting in a tradeoff between signal-to-noise ratio, and acquisition time. In our study, these limitations were partially overcome by carrying out ¹H-MRS experiments at ultra-high magnetic field strength (9.4 T), which improved not only the signal-to-noise ratio but also the spectral resolution. This

enabled a reliable identification of brain metabolites. The use of anatomical markers allowed accurate repositioning between scans and subjects, which limited the variation in partial volumes. In the present study MRS data were stored as a sum of averages instead of individual spectra, therefore post-processing frequency drift corrections could not be applied. In practice we obtained good quality spectra with high reproducibility (between control group at weeks 4, 6 and 12), which were adequately fitted by the LCModel (see [Fig. 1](#) and [Inline Supplementary Figure S1](#)). We would recommend that future studies of ¹H-MRS use post-processing drift corrections as described in more detail by others ([Lange et al., 2011](#); [Near et al., 2014](#); [Tkac and Gruetter, 2005](#); [Tkac et al., 2004](#)). The potential impact of frequency drift on acquired spectra are the following: incoherent signal averaging, which leads to increase in spectral line width, line shape distortions and reduced signal-to-noise ratio ([Near et al., 2014](#)). In addition, severe frequency drift may also limit the ability of LCModel to accurately model spectral line shapes. Differences in frequency drift between time points or between animals may introduce additional uncertainty in metabolite measurements. Performing ¹H-MRS in pathological models, holds an additional risk that observed metabolic changes could be confounded by changes in relaxation time (T2 and T1) of water or metabolites. This effect is further enhanced by using a long TE and short TR ([Bracken et al., 2013](#)). Therefore, we adapted our TE and TR to stay within the suggested limits $TE \leq 35$ ms and $TR \geq 4000$ ms ([Provencher, 2014](#)).

In conclusion, the reversible alterations in brain metabolites of the CPZ mouse model suggest that these metabolites are sensitive indicators to monitor the dynamic CPZ-induced pathologic changes in the brain. As such, these metabolites could be used as neurochemical evidence to study the underlying mechanisms responsible for demyelination, inflammation and axonal suffering and to evaluate the success of potential treatment strategies such as anti-inflammatory/immunomodulatory therapies.

Acknowledgments

This research was supported by research grant FWO-KAN [1521413N](#) (granted to Marleen Verhoye) of the Fund for Scientific Research-Flanders (FWO-Vlaanderen, Belgium), in part by the Flemish Impulse funding for heavy scientific equipment (42/FA010100/1230) (granted to Annemie Van der Linden) and in part by the European Union's Seventh Framework Programme (FP7/2007–2013) under grant agreement n° [278850](#) (INMiND) (granted to Annemie Van der Linden). Jasmien Orije is a holder of FWO-PhD grant. Firat Kara is a holder of FWO post-doctoral fellowship (postdoctoral FWO number: 12S4815N). Caroline Guglielmetti is a holder of an IWT (Institute for the Promotion of Innovation through Science and Technology in Flanders IWT-Vlaanderen) PhD grant. We would like to thank Dr. Simon P. Skinner (University of Leicester, UK) for proofreading.

Conflict of interest

The authors declare no conflict of interest.

Appendix A. Supplementary data

Supplementary data to this article can be found online at <http://dx.doi.org/10.1016/j.neuroimage.2015.04.012>.

References

- Azami Tameh A., Clarner T., Beyer C., Atlasi M.A., Hassanzadeh G. and Naderian H., Regional regulation of glutamate signaling during cuprizone-induced demyelination in the brain, *Ann. Anat.* **195**, 2013, 415–423.
- Bianchi M.C., Tosetti M., Battini R., Manca M.L., Mancuso M., Cioni G., Canapicchi R. and Siciliano G., Proton MR spectroscopy of mitochondrial diseases: analysis of brain metabolic abnormalities and their possible diagnostic relevance, *Am. J. Neuroradiol.* **24**, 2003, 1958–1966.
- Bitsch A., Bruhn H., Vougioukas V., Stringaris A., Lassmann H., Frahm J. and Bruck W., Inflammatory CNS demyelination: histopathologic correlation with in vivo quantitative proton MR spectroscopy, *Am. J. Neuroradiol.* **20**, 1999, 1619–1627.
- Bottomley P.A., Spatial localization in NMR-spectroscopy in vivo, *Ann. N. Y. Acad. Sci.* **508**, 1987, 333–348.
- Boumezbeur F., Mason G.F., de Graaf R.A., Behar K.L., Cline G.W., Shulman G.I., Rothman D.L. and Petersen K.F., Altered brain mitochondrial metabolism in healthy aging as assessed by in vivo magnetic resonance spectroscopy, *J. Cereb. Blood Flow Metab.* **30**, 2010, 211–221.
- Bracken B.K., Rouse E.D., Renshaw P.F. and Olson D.P., T2 relaxation effects on apparent N-acetylaspartate concentration in proton magnetic resonance studies of schizophrenia, *Psychiatry Res.* **213**, 2013, 142–153.
- Bucur A., Bernard A., Cudalbu C., Giraudon P., Graverdonc demilly D., Ratiney H. and Cavassila S., Quantitative analysis of metabolic alterations in a mouse model of neuro-inflammation using in vivo MR Spectroscopy, *Proc. Int. Soc. Magn. Reson. Med.* **16**, 2008, 2179.
- Burg M.B., Kwon E.D. and Kultz D., Regulation of gene expression by hypertonicity, *Annu. Rev. Physiol.* **59**, 1997, 437–455.
- Chard D.T., Griffin C.M., McLean M.A., Kapeller P., Kapoor R., Thompson A.J. and Miller D.H., Brain metabolite changes in cortical grey and normal-appearing white matter in clinically early relapsing–remitting multiple sclerosis, *Brain* **125**, 2002, 2342–2352.

- Choi J.K., Dedeoglu A. and Jenkins B.G., Application of MRS to mouse models of neurodegenerative illness, *NMR Biomed.* **20**, 2007, 216–237.
- Choi J.K., Kustermann E., Dedeoglu A. and Jenkins B.G., Magnetic resonance spectroscopy of regional brain metabolite markers in FALS mice and the effects of dietary creatine supplementation, *Eur. J. Neurosci.* **30**, 2009, 2143–2150.
- Davie C.A., Hawkins C.P., Barker G.J., Brennan A., Tofts P.S., Miller D.H. and McDonald W.I., Serial proton magnetic resonance spectroscopy in acute multiple sclerosis lesions, *Brain* **117** (Pt 1), 1994, 49–58.
- Davies S.E.C., Newcombe J., Williams S.R., McDonald W.I. and Clark J.B., High-resolution proton NMR-spectroscopy of multiple-sclerosis lesions, *J. Neurochem.* **64**, 1995, 742–748.
- De Stefano N. and Filippi M., MR spectroscopy in multiple sclerosis, *J. Neuroimaging* **17** (Suppl. 1), 2007, 31S–35S.
- De Stefano N., Matthews P.M., Ford B., Genge A., Karpati G. and Arnold D.L., Short-term dichloroacetate treatment improves indexes of cerebral metabolism in patients with mitochondrial disorders, *Neurology* **45**, 1995, 1193–1198.
- De Stefano N., Bartolozzi M.L., Guidi L., Stromillo M.L. and Federico A., Magnetic resonance spectroscopy as a measure of brain damage in multiple sclerosis, *J. Neurol. Sci.* **233**, 2005, 203–208.
- Dedeoglu A., Choi J.K., Cormier K., Kowall N.W. and Jenkins B.G., Magnetic resonance spectroscopic analysis of Alzheimer's disease mouse brain that express mutant human APP shows altered neurochemical profile, *Brain Res.* **1012**, 2004, 60–65.
- Denic A., Bieber A., Warrington A., Mishra P.K., Macura S. and Rodriguez M., Brainstem 1H nuclear magnetic resonance (NMR) spectroscopy: marker of demyelination and repair in spinal cord, *Ann. Neurol.* **66**, 2009, 559–564.
- Denic A., Johnson A.J., Bieber A.J., Warrington A.E., Rodriguez M. and Pirko I., The relevance of animal models in multiple sclerosis research, *Pathophysiology* **18**, 2011, 21–29.
- Duarte J.M. and Gruetter R., Characterization of cerebral glucose dynamics in vivo with a four-state conformational model of transport at the blood–brain barrier, *J. Neurochem.* **121**, 2012, 396–406.
- Duarte J.M., Lei H., Mlynarik V. and Gruetter R., The neurochemical profile quantified by in vivo 1H NMR spectroscopy, *NeuroImage* **61**, 2012, 342–362.

- Duarte J.M., Do K.Q. and Gruetter R., Longitudinal neurochemical modifications in the aging mouse brain measured in vivo by 1H magnetic resonance spectroscopy, *Neurobiol. Aging* **35**, 2014, 1660–1668.
- Filippi M., Absinta M. and Rocca M.A., Future MRI tools in multiple sclerosis, *J. Neurol. Sci.* **331**, 2013, 14–18.
- Foos T.M. and Wu J.Y., The role of taurine in the central nervous system and the modulation of intracellular calcium homeostasis, *Neurochem. Res.* **27**, 2002, 21–26.
- Franco-Pons N., Torrente M., Colomina M.T. and Vilella E., Behavioral deficits in the cuprizone-induced murine model of demyelination/remyelination, *Toxicol. Lett.* **169**, 2007, 205–213.
- Gruetter R., Automatic, localized in vivo adjustment of all 1st-order and 2nd-order shim coils, *Magn. Reson. Med.* **29**, 1993, 804–811.
- Gudi V., Moharreh-Khiabani D., Skripuletz T., Koutsoudaki P.N., Kotsiari A., Skuljec J., Trebst C. and Stangel M., Regional differences between grey and white matter in cuprizone induced demyelination, *Brain Res.* **1283**, 2009, 127–138.
- Gustafsson M.C., Dahlqvist O., Jaworski J., Lundberg P. and Landtblom A.M., Low choline concentrations in normal-appearing white matter of patients with multiple sclerosis and normal MR imaging brain scans, *AJNR Am. J. Neuroradiol.* **28**, 2007, 1306–1312.
- Hennig J., Nauerth A. and Friedburg H., RARE imaging: a fast imaging method for clinical MR, *Magn. Reson. Med.* **3**, 1986, 823–833.
- Kipp M., Clarner T., Dang J., Copray S. and Beyer C., The cuprizone animal model: new insights into an old story, *Acta Neuropathol.* **118**, 2009, 723–736.
- Kirov I.I., Tal A., Babb J.S., Herbert J. and Gonen O., Serial proton MR spectroscopy of gray and white matter in relapsing–remitting MS, *Neurology* **80**, 2013, 39–46.
- Kofke W.A., Hawkins R.A., Davis D.W. and Biebuyck J.F., Comparison of the effects of volatile anesthetics on brain glucose metabolism in rats, *Anesthesiology* **66**, 1987, 810–813.
- Kolasinski J., Stagg C.J., Chance S.A., Deluca G.C., Esiri M.M., Chang E.H., Palace J.A., McNab J.A., Jenkinson M., Miller K.L., et al., A combined post-mortem magnetic resonance imaging and quantitative histological study of multiple sclerosis pathology, *Brain* **135**, 2012, 2938–2951.
- Lange T., Zaitsev M. and Buechert M., Correction of frequency drifts induced by gradient heating in 1H spectra using interleaved reference spectroscopy, *J. Magn. Reson. Imaging* **33**, 2011, 748–754.

- Laule C., V. I. M., Kolind S.H., Li D.K.B., Traboulsee T.L., Moore G.R.W. and Mac Kay A.L., Magnetic resonance imaging of myelin, *Am. Soc. Exp. Neurother.* **4**, 2007, 25.
- Lindner M., Heine S., Haastert K., Garde N., Fokuhl J., Linsmeier F., Grothe C., Baumgartner W. and Stangel M., Sequential myelin protein expression during remyelination reveals fast and efficient repair after central nervous system demyelination, *Neuropathol. Appl. Neurobiol.* **34**, 2008, 105–114.
- Lindner M., Fokuhl J., Linsmeier F., Trebst C. and Stangel M., Chronic toxic demyelination in the central nervous system leads to axonal damage despite remyelination, *Neurosci. Lett.* **453**, 2009, 120–125.
- Lucchinetti C., Bruck W., Parisi J., Scheithauer B., Rodriguez M. and Lassmann H., Heterogeneity of multiple sclerosis lesions: implications for the pathogenesis of demyelination, *Ann. Neurol.* **47**, 2000, 707–717.
- Lucchinetti C.F., Parisi J. and Bruck W., The pathology of multiple sclerosis, *Neurol. Clin.* **23**, 2005, 77–105, (vi).
- Lukovic D., Valdes-Sanchez L., Sanchez-Vera I., Moreno-Manzano V., Stojkovic M., Bhattacharya S.S. and Erceg S., Brief report: astrogliosis promotes functional recovery of completely transected spinal cord following transplantation of hESC-derived oligodendrocyte and motoneuron progenitors, *Stem Cells* **32**, 2014, 594–599.
- Mader I., Roser W., Kappos L., Hagberg G., Seelig J., Radue E.W. and Steinbrich W., Serial proton MR spectroscopy of contrast-enhancing multiple sclerosis plaques: absolute metabolic values over 2 years during a clinical pharmacological study, *Am. J. Neuroradiol.* **21**, 2000, 1220–1227.
- Mandal P.K., In vivo proton magnetic resonance spectroscopic signal processing for the absolute quantitation of brain metabolites, *Eur. J. Radiol.* **81**, 2012, e653–e664.
- Marjanska M., Curran G.L., Wengenack T.M., Henry P.G., Bliss R.L., Poduslo J.F., Jack C.R., Jr., Ugurbil K. and Garwood M., Monitoring disease progression in transgenic mouse models of Alzheimer's disease with proton magnetic resonance spectroscopy, *Proc. Natl. Acad. Sci. U. S. A.* **102**, 2005, 11906–11910.
- Mason J.L., Jones J.J., Taniike M., Morell P., Suzuki K. and Matsushima G.K., Mature oligodendrocyte apoptosis precedes IGF-1 production and oligodendrocyte progenitor accumulation and differentiation during demyelination/remyelination, *J. Neurosci. Res.* **61**, 2000, 251–262.

- Mason J.L., Langaman C., Morell P., Suzuki K. and Matsushima G.K., Episodic demyelination and subsequent remyelination within the murine central nervous system: changes in axonal calibre, *Neuropathol. Appl. Neurobiol.* **27**, 2001, 50–58.
- Matsushima G.K.M.P., The neurotoxicant, cuprizone, as a model to study demyelination and remyelination in the central nervous system, *Brain Pathol.* **11**, 2001, 10.
- Morell P., Barrett C.V., Mason J.L., Toews A.D., Hostettler J.D., Knapp G.W. and Matsushima G.K., Gene expression in brain during cuprizone-induced demyelination and remyelination, *Mol. Cell. Neurosci.* **12**, 1998, 220–227.
- Near J., Edden R., Evans C.J., Paquin R., Harris A. and Jezzard P., Frequency and phase drift correction of magnetic resonance spectroscopy data by spectral registration in the time domain, *Magn. Reson. Med.* 2014, <http://dx.doi.org/10.1002/mrm.25094>.
- Oh J., Pelletier D. and Nelson S., Corpus callosum axonal injury in multiple sclerosis measured by proton magnetic resonance spectroscopic imaging, *Arch. Neurol.* **61**, 2004, 1081–1086.
- Oz G., Nelson C.D., Koski D.M., Henry P.G., Marjanska M., Deelchand D.K., Shanley R., Eberly L.E., Orr H.T. and Clark H.B., Noninvasive detection of presymptomatic and progressive neurodegeneration in a mouse model of spinocerebellar ataxia type 1, *J. Neurosci.* **30**, 2010, 3831–3838.
- Pascual J.M., Solivera J., Prieto R., Barrios L., Lopez-Larrubia P., Cerdan S. and Roda J.M., Time course of early metabolic changes following diffuse traumatic brain injury in rats as detected by (1)H NMR spectroscopy, *J. Neurotrauma* **24**, 2007, 944–959.
- Pfeuffer J., Tkac I., Provencher S.W. and Gruetter R., Toward an in vivo neurochemical profile: quantification of 18 metabolites in short-echo-time H-1 NMR spectra of the rat brain, *J. Magn. Reson.* **141**, 1999, 104–120.
- Provencher S.W., Estimation of metabolite concentrations from localized in-vivo proton NMR-spectra, *Magn. Reson. Med.* **30**, 1993, 672–679.
- Provencher S.W., Automatic quantitation of localized in vivo 1H spectra with LCModel, *NMR Biomed.* **14**, 2001, 260–264.
- Provencher S.W., LCModel & LCMgui user's manual, <http://s-provencher.com/pages/lcm-manual.shtml> 2014.
- Ramadan S., Lin A. and Stanwell P., Glutamate and glutamine: a review of in vivo MRS in the human brain, *NMR Biomed.* **26**, 2013, 1630–1646.
- Saneto R.P., Friedman S.D. and Shaw D.W., Neuroimaging of mitochondrial disease, *Mitochondrion* **8**, 2008, 396–413.

- Sijens P.E., Mostert J.P., Oudkerk M. and De Keyser J., (1)H MR spectroscopy of the brain in multiple sclerosis subtypes with analysis of the metabolite concentrations in gray and white matter: initial findings, *Eur. Radiol.* **16**, 2006, 489–495.
- Skripuletz T.G.V., Hackstette D. and Stangel M., De- and remyelination in the CNS white and grey matter induced by cuprizone: the old, the new, and the unexpected, *Histol. Histopathol.* **26**, 2011, 13.
- Srinivasan R., Sailasuta N., Hurd R., Nelson S. and Pelletier D., Evidence of elevated glutamate in multiple sclerosis using magnetic resonance spectroscopy at 3 T, *Brain* **128**, 2005, 1016–1025.
- Stidworthy M.F., Genoud S., Suter U., Mantei N. and Franklin R.J.M., Quantifying the early stages of remyelination following cuprizone-induced demyelination, *Brain Pathol.* **13**, 2003, 329–339.
- Tkac I. and Gruetter R., Methodology of H NMR spectroscopy of the human brain at very high magnetic fields, *Appl. Magn. Reson.* **29**, 2005, 139–157.
- Tkac I., Starcuk Z., Choi I.Y. and Gruetter R., In vivo H-1 NMR spectroscopy of rat brain at 1 ms echo time, *Magn. Reson. Med.* **41**, 1999, 649–656.
- Tkac I., Henry P.G., Andersen P., Keene C.D., Low W.C. and Gruetter R., Highly resolved in vivo 1H NMR spectroscopy of the mouse brain at 9.4 T, *Magn. Reson. Med.* **52**, 2004, 478–484.
- Tkac I., Dubinsky J.M., Keene C.D., Gruetter R. and Low W.C., Neurochemical changes in Huntington R6/2 mouse striatum detected by in vivo 1H NMR spectroscopy, *J. Neurochem.* **100**, 2007, 1397–1406.
- Tourbah A., Stievenart J.L., IbaZizen M.T., Zannoli G., LyonCaen O. and CabanisE.A., In vivo localized NMR proton spectroscopy of normal appearing white matter in patients with multiple sclerosis, *J. Neuroradiol.* **23**, 1996, 49–55.
- Venturini G., Enzymic activities and sodium, potassium and copper concentrations in mouse brain and liver after cuprizone treatment in vivo, *J. Neurochem.* **21**, 1973, 1147–1151.
- Xie M.Q., Tobin J.E., Budde M.D., Chen C.I., Trinkaus K., Cross A.H., McDanielD.P., Song S.K. and Armstrong R.C., Rostrocaudal analysis of corpus callosum demyelination and axon damage across disease stages refines diffusion tensor imaging correlations with pathological features, *J. Neuropathol. Exp. Neurol.* **69**, 2010, 704–716.
- Xuan Y., Yan G., Peng H., Wu R. and Xu H., Concurrent changes in 1H-MRS metabolites and antioxidant enzymes in the brain of C57BL/6 mouse short-termly exposed to cuprizone: possible implications for schizophrenia, *Neurochem. Int.* **69**, 2014, 20–27